IEEE Access
Multidisciplinary ⋮ Rapid Review ⋮ Open Access Journal

Received 16 September 2023, accepted 3 October 2023, date of publication 13 October 2023, date of current version 23 October 2023.

Digital Object Identifier 10.1109/ACCESS.2023.3324417

RESEARCH ARTICLE

Arm-Mounted Assistive Robot for Measuring Contact Force and Evaluating Wearer Safety

SHINICHI MASAOKA, (Member, IEEE), YUKI FUNABORA, (Member, IEEE), AND SHINJI DOKI, (Senior Member, IEEE)

Department of Information and Communication Engineering, Graduate School of Engineering, Nagoya University, Chikusa-Ku, Nagoya, Aichi 464-8601, Japan

Corresponding authors: Shinichi Masaoka (masaoka.shinichi@nagoya-u.jp) and Yuki Funabora (funabora.yuki.f3@f.mail.nagoya-u.ac.jp)

This work was supported by the Japan Society for the Promotion of Science (JSPS) KAKENHI under Grant 16H05915 and Grant 20H04564, and in part by Tobe Maki Scholarship Foundation.

This work involved human subjects or animals in its research. Approval of all ethical and experimental procedures and protocols was granted by the Ethics Committee with the Faculty of Engineering, Nagoya University, under Application No. 19-7.

ABSTRACT We developed a wearable assistive robot that directly measures the contact force acting between the robot and the human body, aiming to enhance the safety of such wearable devices. The force acting on the body is not directly measured, instead, it is estimated by measuring the torque acting on the robot joint in the wearable assistive robot. Despite the risk of failing to recognize dangerous forces due to modeling errors, the forces actually at work have not been examined. Here, we developed an arm-mounted assistive robot that directly measures the contact force as the distribution information to build a system and evaluate safety; in addition, the contact state between the robot and the human body was discussed. Accordingly, two experiments were conducted with 10 subjects. The first verified the contact force measurement performance of the robot, while the second demonstrated the application of contact force information to check the safety of the robot. The proposed robot can accurately measure the contact force, and the robot movement is safe under general control, for example, using the pain tolerance limit as the safety index. This eliminated the risk of not directly monitoring the forces acting on the surface of the human body. Furthermore, our result have implication for evaluating structural problems of the robot by evaluating contact conditions during movements.

INDEX TERMS Assistive robot, contact force distribution, exoskeleton, wearable robot.

I. INTRODUCTION

Wearable assistive robots, which are devices directly attached to the human body to assist in several tasks, are garnering significant attention in several fields, such as rehabilitation, nursing care, transportation, and agriculture [1], [2]. Currently, wearable assistive robots are being developed to enhance physical function and reduce physical burden.

HAL [3], a wearable assistive robot in nursing care developed by Cyberdyne, is a physical extension example. HAL employs electromyography (EMG) sensors to predict the wearer's movements. It supports the wearer's movements by calculating the necessary torque required to enhance the physical functions of patients with weakened muscles and nerve paralysis. For the elderly, it is crucial to prevent musculoskeletal disorders and circumvent the need for nursing care by undergoing appropriate rehabilitation after these disorders emerge. In Japan and other advanced countries with aging populations [4], there are increasing expectations for wearable assistive robots to help prevent the progression from musculoskeletal disorders to a state requiring nursing care.

Muscle suits [5] are robots designed to reduce the physical burden. The McKibben-type artificial muscle, characterized by its flexibility, lightweight, and high power, is utilized as an actuator and can exert an assist force of approximately 30 kgf. When the switch is pressed, the artificial muscles attached to the muscle suit exert an assist force, and the suits reduce the physical burden on the wearer. As aforementioned,

The associate editor coordinating the review of this manuscript and approving it for publication was Yang Tang.

various robots are being researched and developed, and their application in the real world is being promoted.

In this field, developing a framework that can measure and control the force applied to the wearer by the robot is crucial. This is because these wearable assistive robots transmit force to the wearer via direct contact; hence, unexpected excessive force may injure the wearer. Kong et al. [6] proposed a joint torque feedback control system that measures the force applied by the robot to the wearer as the torque of the robot joints (motors) and controls the robot to eliminate deviation from the torque command. At the torque level, a framework to measure and control the force applied to the wearer on the rotational axis has been established. However, this method does not directly measure the force applied by the robot on the wearer and the robot may cause harm to the human body. For example, when the contact location is close to the joint, a large risk force capable of injuring the wearer will be measured as a small torque; hence, the robot cannot identify potential hazards. In addition, the torque sensor built into the motor cannot measure the twisting force exerted on the robot joint and another safety index is required.

This study focuses on measuring and evaluating the contact force between the wearable assistive robot and human body following a general wearable robot configuration, but with contact sensors, and using the existing control method. We employ the directly measured contact force, instead of the estimated value obtained from the joint torque, for safety assessment and to improve the safety management performance of wearable assistive robots. Accordingly, we developed a robot that directly measures the contact force between the robot and wearer. By attaching contact distribution sensors to the contact surface between the robot and human body, the robot can directly measure the contact force exerted by the robot on the human body. This system enables visualizing the contact force per small contact area as a surface distribution, which is yet to be adequately discussed in conventional robots. We conducted two experiments with 10 subjects involving a dumbbell lifting exercise while assisted by a wearable assistive robot. The first experiment verified the contact force measurement performance of the robot, and the second demonstrated the application of contact force information to check the safety of the robot. Consequently, we verified that the proposed robot can accurately measure the contact force and demonstrated that the robot movement is safe under general control using pain tolerance limit as the safety index.

The contribution of this paper is threefold. First, we developed a robot that directly measures the contact force distribution between the robot and human body. Second, the application of contact force information was demonstrated in evaluating the safety of the control method in terms of the pain tolerance limit, in addition to the general safety management framework. Third, we inferred that the contact force distribution information can help evaluate structural problems. Third contribution is also a practical implication suggested by the experimental results. These findings contribute to improving the safety management performance of conventional wearable robots. We believe that safety evaluation in research on the latest wearable assistive robots should be based on actual contact forces measured directly.

II. RELATED WORK

Various sensors have been proposed for the development of wearable robots. In general, the following sensors are mounted on a wearable robot for safety management or control purposes: torque sensors, force sensors, inertial measurement unit, and electromyography sensors. Torque sensors have been used for a long time, but it is difficult to perform rigorous control and measurement with torque information alone; hence, they are often used in combination with other sensors in recent research. Force sensors are also used in many robots, but often as switches to trigger something and do not directly contribute to measurement. Inertial measurement units and electromyography sensors have long been used in combination with joint sensors to estimate the state of the human body and robot. We summarize the characteristics, purpose of use, and limitations of these sensors for the safety assessment performance.

One of the simplest configurations is the robot using joint sensors [7], [8], [9], [10], [11], [12], [13]. As this robot is originally mounted on an actuator, it does not require additional sensors. When measuring positions in a redundant system, a robot can be stopped by detecting mounting misalignment [13]. In addition, measuring torque enables feedback control, as described in a [6], and its applications also exist in impedance control [8]. However, they are only used in robot joints.

Some robots are equipped with force sensors to directly measure force [14], [15], [16], [17], [18], [19], [20], [21]. Such robots focus on human interactions, as they directly measure applied force. By employing a force sensor, the robot's posture can be controlled by admittance control [16]. However, this sensing offer minimal control and contact conditions cannot be comprehensively observed. Regarding force sensors, foot sensors are often used in lower-limb robots [22], [23], [24]. These sensors measure idle time or trigger assist torque timing and do not contribute to safety. D. Sanz-Merodio's robot differs from the others in that although its foot force is measured by distribution, it is employed for control and analysis and does not measure assist forces or improve safety.

Inertial measurement unit sensors are commonly used sensors, especially in lower limb robots [23], [25], [26], [27], [28], [29]. They are used to observe falls and analyze robot behavior; however, using them to manage safety and prevent hazards is challenging.

EMG sensors are another typical sensor type. By measuring the muscle load, the robot's assist performance can be evaluated [29], [30], [31]. Although there have been attempts to employ them for control [3], [32], EMG sensors have low

reproducibility [33], and several related issues need to be addressed.

Finally, wearable robots that are not joint-driven are described. These robots apply air pressure to cylinders to drive their joints [34], [35]. The exerted force and joint angle are calculated from the internal pressure and distance of the cylinder; however, this robot does not differ from other robots in that interaction forces are not measured directly. Owing to the advancement of soft actuators, robots with McKibben artificial muscles have also been developed [36]. However, these robot types cannot directly sense the exact force applied to the device and wearer. Thus, the robot proposed in [36] only assures safety by physically restricting the range of motion.

Therefore, in conventional assistive robots, sensors are often used to control or evaluate the model and analyze the experiments. Even in safety-conscious research, no robot can observe every contact area. This research will measure the forces acting between the wearer and robot area as the distribution information and visualize the wearing condition to evaluate the robot's safety. This could be an effective means of evaluating the effectiveness of assistive robots and the safety of robots with soft actuators, whose interactions are difficult to measure.

III. FABRICATION OF A ROBOT FOR MEASURING CONTACT FORCE

This section identifies the design requirements for the robot employed in this study. We then describe the robot specifications that satisfy these requirements.

First, we consider a robot mechanism for the flexion-extension motion of the elbow to explore measurement possibilities as a basic study. Because linear and twisting motions were ignored in this study, this exoskeleton robot solely models the flexion-extension motion as the single-axis rotational joint. In particular, the silicone in the rigid frame is positioned significantly close to the human body to measure the contact force.

A. REQUIREMENTS OF ROBOT

The design of the link part is important for the robot to measure the contact force and transmit the assist force. Hence, the requirements are divided into two main categories: structures to measure the contact force for safety evaluation and transmit the exerted motor power to the forearm. Here, we propose a three-layer link configuration to satisfy the contact, sensor, and frame section requirements (Fig.1).

1) CONTACT SECTION

The contact section measures the contact force and evaluates safety. Here, the contact force should be measured without spatial mounting misalignment or absence of time series. Accordingly, the shape of the inner contact section and human body surface should match. Hence, the shape is designed based on statistical data [37] obtained from human body shape measurements.

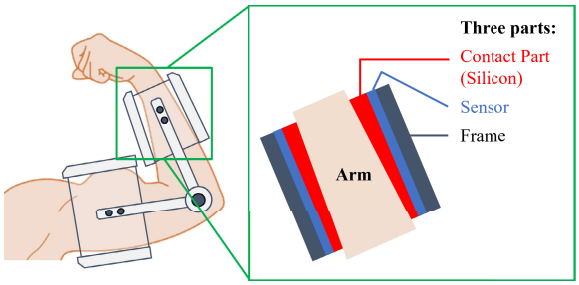

FIGURE 1. Configuration of arm-mounted assistive robot: The robot frame consists of a hard outer layer, middle sensor layer, and soft inner silicone layer.

TABLE 1. Contact distribution sensor specifications.

Spatial Resolution $[mm^2]$	20×20
Measuring Period [s]	0.05
Max Pressure [N]	10.7

Based on the FY2017 Physical Fitness and Exercise Survey conducted by the Japan Sports Agency [38], the average body shape of an adult male is 171.6 cm in height and 65.7 kg in weight. DhaibaWorks [37] was used to generate the human model for the previous body shape, and the arm shape was cut out. The contact section was made from 3D-printed silicone of thickness 3.8-14.8 mm.

2) SENSOR SECTION

The sensor section measures the contact force generated by the wearer's arm movement as absolute values and distribution information. Absolute values are required to evaluate whether the measured value is dangerous; in addition, it can be adopted as a threshold for physical quantities when using indicators. Distribution information comprehensively estimates the contact state between the robot and human body, unlike the torque of one-dimensional information; thus, the degree of stress concentration can be visualized.

In addition, sensors cover the entire contact area between the robot and human body and are attached all over the frame's interior. Here, we employed the commercially available SR Softvision (numerical version) [39], [40] sensors.

Table 1 presents the specifications of the contact distribution sensor. In each upper arm and forearm link, two sheet-type contact distribution sensors with 5×5 cells were placed, one each on the palmar and dorsal sides. The sensor cells were placed inside the cylindrical rigid outer frame without any gaps.

3) FRAME SECTION

The frame section should transmit the exerted torque of the motor to the forearm of the wearer as the assistive force; hence, a rigid material was selected. In addition, a cylindrical structure covering the flexible contact part was adopted to maintain a constant deformation rate on the attached sensor and measure a uniform contact force.

TABLE 2. HEBI robotics X5-9 specifications.

Peak Torque [Nm]	13
Cont. Torque [Nm]	9
Max Speed [rpm]	14
Angular Resolution [°]	0.005
Torque Resolution [Nm]	0.01

The frame was fabricated using a 3D printer (Markforged Mark Two) that uses a mixture of nylon and carbon fibers to create a lightweight, highly rigid frame. The length of the forearm and upper arm links was set at 100 mm. A 90 mm gap between the forearm and upper arm links ensures the wearer's motion. Adjustable parts were prepared to accommodate individual differences in arm diameter. The inner diameter of the frame could be adjusted to 120, 125, or 130 mm, depending on the wearer. Each layer was printed 0.1 mm thick.

The frames for the forearm and upper arm are connected with the motor for the joint part, HEBI Robotics X5-9, which is compact, has high power, and can input torque and position. Table 2 presents the specifications of the motor.

B. SPECIFICATIONS OF THE MANUFACTURED ROBOT

Figure 2 illustrates the fabricated robot and the robot attached to the arm. The extended total length of the robot is 400 mm, and its weight is 2.3 kg. The total contact force distribution of the upper arm and forearm links is measured for 100 cells (each cell is 400 mm^2). The controller was implemented in C on a general-purpose computer (CPU: Intel(R) Xeon(R) CPU E5-2670 v3, Memory: 64.0 GB). The control cycle was set to 50 ms, equal to the shortest sensor measurement cycle.

IV. VALIDATION OF CONTACT FORCE DISTRIBUTION MEASUREMENTS

We verify whether this robot can accurately measure the contact force. Because we could not directly evaluate the measurement accuracy, we assessed the robot's validity from two perspectives. First, we qualitatively verify aligning the relationship between the wearer's motion and the transition of the measured force distribution. Second, we quantitatively evaluate and validate the accuracy of the measured force value by adopting the torque-based control [6], a conventional control method.

First, the distribution transition's validity was verified based on two qualitative considerations: whether the expected force distribution for the wearer's motion was measured and whether the reproducibility was observed.

In the quantitative evaluation, the distributed contact force was converted to joint torque $\hat{\tau}_{sensor}$ and compared to the torque sensor (τ_{sensor}) value built into the motor. $\hat{\tau}_{sensor}$ is calculated using (1) (refer to Fig. 3).

$$\hat{\tau}_{sensor} = \sum_i F(i)l(i) \tag{1}$$

where $l(i)$ represents the moment arm from the joint axis to the center position of the sensor cell in row i (on the O axis).

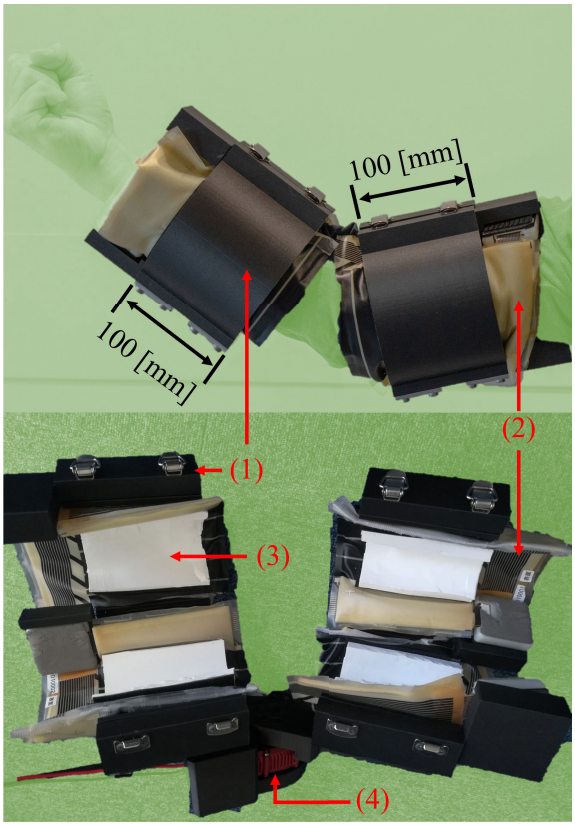

FIGURE 2. Developed wearable assistive robot for arm: (1) 3D printed robot frame, (2) sheet-type contact distribution sensor (SR sensor), (3) contact section designed via DhaibaWorks, (4) actuator (HEBI X-9).

$F(i)$ is calculated as

$$F(i) = \sum_j sP(i,j)cos(\phi_j) \tag{2}$$

Equation (2) defines the degenerated force on the O-axis of the pressure measurement $P(i,j)$ on the j-th sensor cell in row i. s denotes the area(m^2) of the sensor cell while ϕ_j represents the angle between the normal vector of the sensor cell in row j and the dorsal direction ($j = 3$).

A. IMPLEMENTED CONTROL METHOD

Figure 4 presents an overview of the proposed control method based on joint torque.

Proportional control, the most basic control method, was employed because this experiment aimed to evaluate the measured value and not the control performance. The exerted motor torque was determined, such that the deviation τ_{error} between the torque command value τ_{ref} and sensor value τ_{sensor} obtained from the torque sensor was minimized. The sensor measures the exerted torque τ_{output} before F_{output}, the transmitted assist force generated by the actuator via the robot frame. Hence, although it can manage the torque condition, it cannot control the actual assist forces F_{output} or F_{assist}. K_τ in Fig. 4 represents the P gain. F_{output} generated by the frame acts on the human body to alter the wearer's posture $\phi_{humanbodyjoint}$.

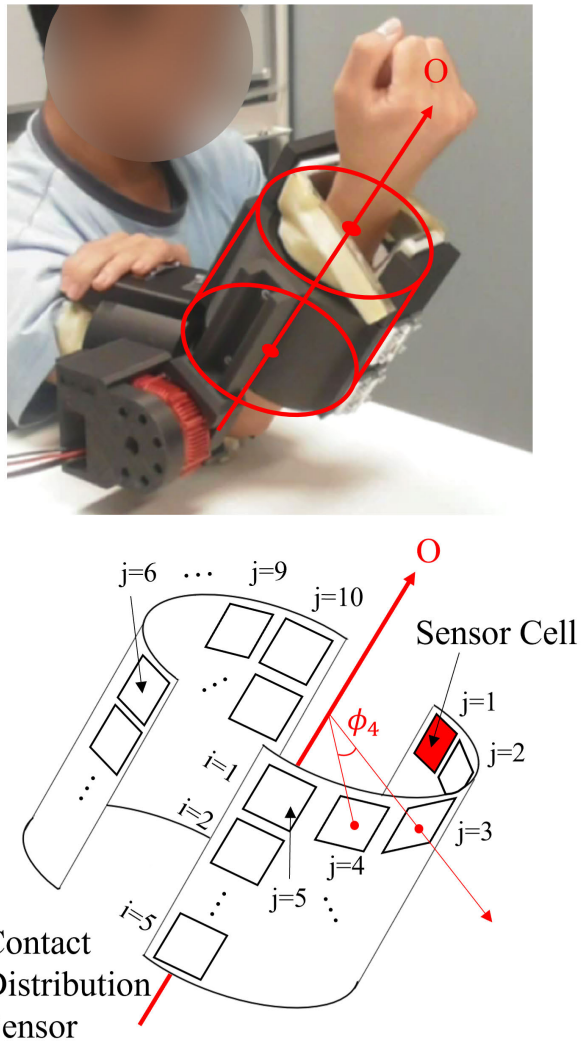

FIGURE 3. Coordinate axes and sensor cell definition: The longitudinal direction of the forearm is defined as the O-axis. The sensor cell is defined as i along the O-axis and j in the arm circumference direction. ϕ_j represents the angle between the normal vector of the sensor cell in row j and the dorsal direction ($j = 3$).

B. EXPERIMENTAL CONDITIONS

The experiments, approved by the Ethics Committee with the Faculty of Engineering, Nagoya University, were conducted with 10 male adult participants. A DC power supply (Meanwell ESP20-480-24) was used to power the motor. Throughout this experiment, the participants remained seated on a chair. First, the participant put on the robot and fixed it such that the entire lower surface of the upper arm touched the desk. The radius of the frame section was adjusted according to the tightness and comfort level of the participants before the experiment. The arm angle θ was defined as the angle between the ground and forearm, with the fully extended arm at 0° (initial state; Fig. 5). During the experiment, the participant performs movements while looking at the screen, as displayed on the right side of Fig. 5. The same movements were reproduced as much as possible between participants by referring to the robot's current and reference positions that move at a constant velocity to the desired angle in 3 s. The participant initially held a 2 kg dumbbell and repeated the following motions five times.

(i) Hold $\theta = 0°$ for 3 s
(ii) Bend arms until $\theta = 60°$ over 3 s
(iii) Hold at $\theta = 60°$ for 3 s
(iv) Extend arms until $\theta = 0°$ over 3 s

In (ii) and (iv), the current and target elbow angles were presented to the participants such that they could move their arms at a constant speed (refer to Fig. 5). During the movements, the torque command value was set to $\tau_c = 6$ for movements (i), (ii), and (iii), requiring an enormous exertion of muscular force, and $\tau_c = 1$ for movement (iv), requiring a relatively small exertion force. The forearm's length is approximately 0.35 m, with a 2 kg dumbbell corresponding to a 6.86 Nm load on the wrist. The amount of assistance corresponds to 87% of the load in (i), (ii), and (iii), and 15% of the load in (iv).

C. RESULTS

1) QUALITATIVE VERIFICATION

Figures 6 and 7 present the forearm contact force distributions obtained for Participants E and B. The participants repeated the experimental motion five times; however, we illustrate only the third cycle because of their reproducibility within the same subject. Fully extended, bending, fully bent, and extending correspond to motions (i), (ii), (iii), and (iv), respectively. Figure 6 presents the results of the participant closest to the standard body shape (BMI 22.8), while Fig. 7 presents the results of the participant farthest from the standard body shape (BMI 17.3). A similar transition in contact force distribution is observed in the two participants regardless of their body shape. Moreover, the force on the wrist side is more significant than that on the elbow side. This difference is believed to be because the silicone in the contact area sinks deeper as it gets closer to the wrist, for there is no mechanism to support the wrist when handling the dumbbell. The distribution was widespread over $i = 1, \ldots, 4$ in extension (24, 25, 26 s) while it concentrated around $i = 1$ in flexion (30, 31, 32 s). Owing to the silicone's flexibility, the movements were not perfectly synchronized between the robot and human body. This may have caused the silicone above the sinking level to be more pronounced in flexion than in extension. The same result was observed in other participants. The transition of the contact force distribution was practical for the motion, although bias during the motion was observed for the above reasons.

2) QUANTITATIVE VERIFICATION

Figures 8(a) and 8(b) present the τ_{sensor} and $\hat{\tau}_{sensor}$ values obtained during the exercise, respectively.

The horizontal and vertical axes represent time (s) and torque (Nm), respectively. The solid line and shaded area represent the mean and standard deviation for the ten subjects, respectively.

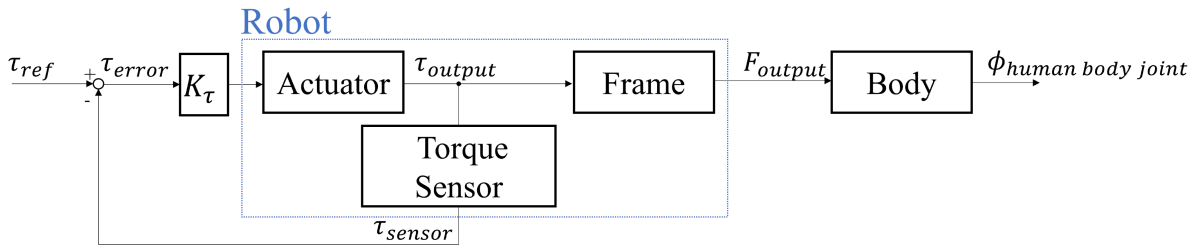

FIGURE 4. Signal flow of torque-based control: τ_{ref} is the torque command value. τ_{sensor} is the sensor value obtained from the torque sensor. τ_{error} is the deviation between τ_{ref} and τ_{sensor}. τ_{output} is the exerted torque. τ_{output} is transformed to F_{output}, the contact force the frame exerts on the human body via the robot frame. $\phi_{humanbodyjoint}$ is the wearer's posture. Proportional control was employed and K_τ represents the gain.

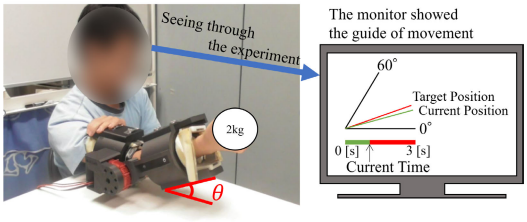

FIGURE 5. Experiment and guide screen displayed to participants: The subject performs a 2 kg dumbbell lifting exercise. The subject moves the arm while watching the guide monitor. The guide monitor shows the current position (green), target position (red), and current time relative to the robot movement angle during the experiment. The target position moves 60° for 3 s at a constant velocity during the bend and extend motions.

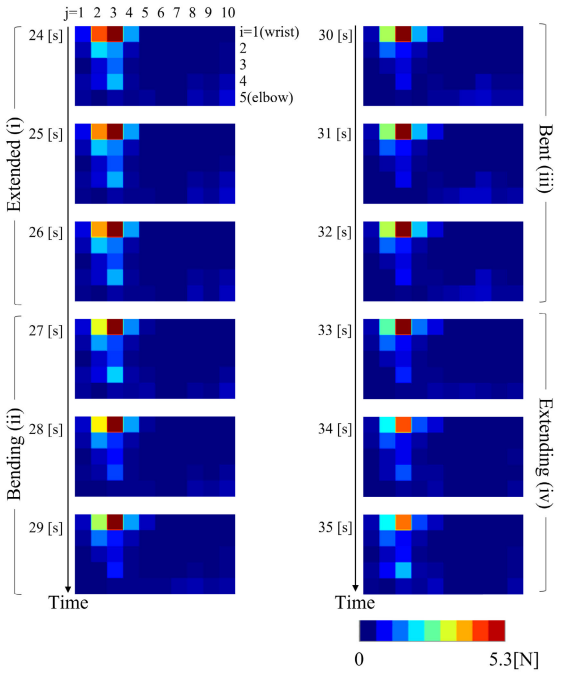

FIGURE 6. Transition of contact force distribution by torque-based control (Participant E, BMI: 22.8).

Figure 8(a) indicates that the implemented torque-based control is functional, tracking approximately 6 and 1 Nm in (i) and (iii), respectively. Figure 8(b) also demonstrates that (i) and (iii) can be followed by 6 and 1 Nm, respectively. The standard deviation is larger than that in Fig. 8(a); however, the average value is similar to the actual value.

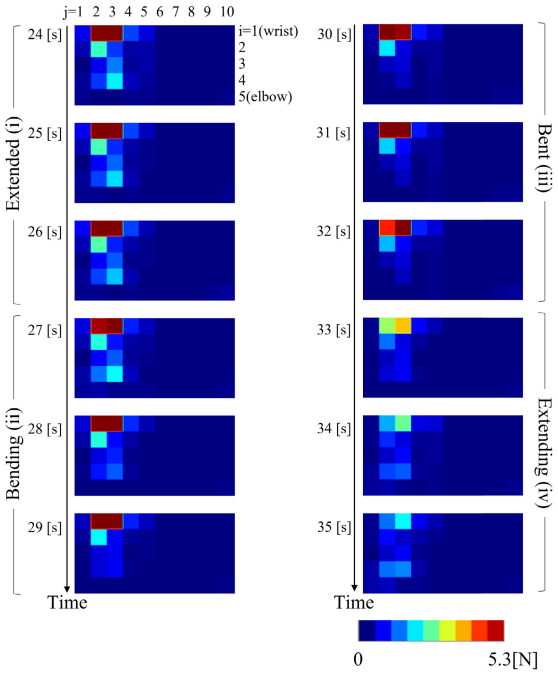

FIGURE 7. Transition of contact force distribution by torque-based control (Participant B, BMI: 17.3).

The time average of the absolute difference between τ_{sensor} and $\hat{\tau}_{sensor}$ for all participants was 0.592 Nm. Because the moment arm from the elbow joint of the robot to the contact sensor is approximately 150 mm, the error amount of the force at the average position of the sensor cell was estimated to be 0.09 N. The measurement noise generated in the contact sensor cell was approximately 0.05 N in standard deviation based on the preliminary measurement; hence, the error is considered to be triggered by the measurement resolution of the contact sensor. Contact force distribution allows for the calculation of torque values that are close to the actual values, demonstrating the requisite measurement performance for safety evaluations.

V. SAFETY EVALUATION USING CONTACT FORCE DISTRIBUTION

We demonstrate the application of the contact force distribution information and verify the safety of the robot and controls based on the contact force values and distribution.

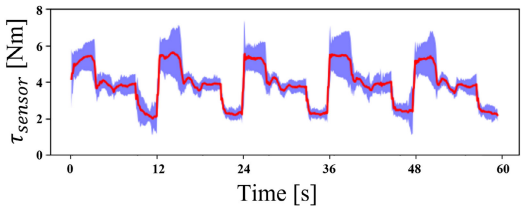

(a) Torque measured by the torque sensor

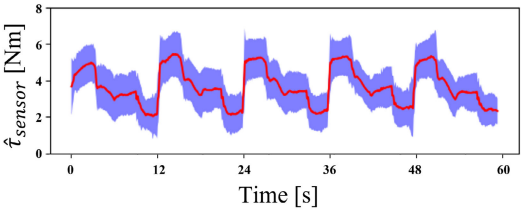

(b) Torque calculated from the contact force

FIGURE 8. Time series of joint torque from torque and contact sensors.

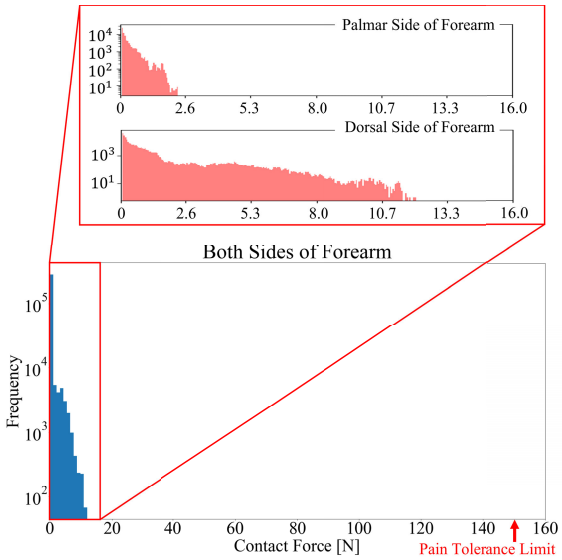

FIGURE 9. Frequency of contact force appearance throughout all experiments (torque-based control): frequencies of both sides of the forearm (blue) indicate that all measurements are significant under the pain tolerance limit for all participants. Results on the palmar and dorsal sides indicate that large contact forces work on the dorsal side.

Here, the safety of the general torque-based control was verified using the dumbbell lifting experiment described above. First, the transitions in the contact force distribution were observed to confirm the emergence of discontinuous and sudden forces. An excessive force exerted abruptly suggests a structural defect or control breakdown. Second, histograms of the contact forces measured during the experiment were presented. The results demonstrated that the robot operated at a significantly small level compared to the pain tolerance limit.

A. CONTACT DISTRIBUTION TRANSITION

For safety evaluation, the results from Figs. 6 and 7 were employed. In both figures, contact distribution transitioned continuously in time and space; hence, no unexpected intermittent force is observed, allowing the safe and smooth operation of the robot. The result was similarly verified for all participants. However, although a constant force concentration is observed near the wrist, the distribution information does not numerically ascertain whether this force is harmful. Consequently, this is discussed in the next section.

The developed robot was designed to imitate the structure of human arms and can move in perfect synchrony with the human body by managing only the joint torque ideally. Consequently, the robot moved smoothly, even on the general control.

Thus, it was verified that the torque-based control was safe based on the appropriate robot design by analyzing the contact force distribution.

B. ASSESSMENT OF SAFETY BY CONTACT FORCE

Figure 9 presents the frequency distribution of the contact force magnitude generated in each sensor cell during the experiment. The horizontal and vertical axes represent the contact force magnitude and frequency of occurrence, respectively. The upper and lower panels present the palmar ($j = 1, \ldots, 5$) and dorsal ($j = 6, \ldots, 10$) sides, respectively. Although a few differences exist in the measured contact force magnitudes, the two control results are almost equivalent, as described in the following paragraphs.

In Fig. 9, the lower panel has a larger contact force than the upper panel. This is because the contact force on the dorsal side is more significant than that on the palmar side, owing to the dumbbell load. Regarding safety, Fig. 9 demonstrates that the maximum contact force is approximately 12 N. This force is significantly lower than the arm's pain tolerance limit of approximately 150 N [41]. This result implies that the 87% assistance for a 2 kg dumbbell load is safe even with existing methods.

The obtained results indicate that the contact force distribution measurement is beneficial from the perspective of safety evaluation and the control is actually safe.

VI. DISCUSSION

In addition to safety evaluation, contact force distribution was employed to investigate the inherent structural problems of the proposed robot. The previous experiment revealed unevenly distributed contact force around the dorsal wrist ($i = 1, j = 3$) and palmar elbow ($i = 5, j = 7$). Although it was verified in the chapter V-B that the robot and control method are safe, the firmly contacted and half-floating parts in the robot link limit robot assistance.

Although other reasons can be considered, the primary cause of this phenomenon could be as follows. The design objective of the proposed robot was to measure the contact force without any leakage; hence, silicone contact parts were used to fit the body evenly. However, silicone deformation can generate significant stress, as described in the experiment. In addition, the deformation of the flexible contact section is difficult to consider in the design phase. The results obtained

from the contact force distribution suggest the need for a wrist support mechanism in arm-mounted assistive robots for performance improvement. Hence, measuring contact force distribution is beneficial for evaluating safety and contact conditions during movements.

However, it is unreasonable to conclude that this sensor can achieve complete safety management as only vertical contact forces are measured and not the shear forces. Therefore, the frictional force that could cause the attachment to shift has not been measured. A sensor that can handle such forces is required for more advanced observation of contact conditions. Furthermore, current sensor technologies are still emerging; therefore, sensors with faster measurement cycles must be developed to achieve practical operating speeds.

Furthermore, a simple structure was considered because the robot was designed to measure the contact force directly. In addition, the obtained contact force distribution is within the expected range, although it is worth proving with actual measurements. Moreover, if the robot can imitate the structure of the human body, it is structurally difficult to measure and discuss unknown contact force distributions. For example, in assistive robots targeting the torso, motion is approximated by reducing the number of robot joints relative to the number of human body joints. Conventional methods of estimating contact state from joints are difficult to apply to multi-joint robots as the joint angles between the human body and robot are not uniquely linked. Using such multi-joint robots could increase the practical value of our method.

VII. CONCLUSION

Conventional wearable robots estimate contact conditions based on joint information for safety management and control. Even if the robot is equipped with a force sensor, a point sensor that cannot provide distribution information is employed. Our robot can directly visualize and evaluate the contact state by attaching a force sensor that measures the contact force between the robot and human body as a distribution.

We designed and fabricated an arm robot that directly measures contact forces to improve the safety of wearable assistive robots and provides a novel approach to evaluate the robot's safety. An experiment using test participants verified that the robot could measure the contact force distribution information during the robot's motion. In addition, we demonstrated that the contact force distribution information is beneficial in evaluating the safety of the robot; for example, the robot's safety can be ascertained by adopting a conventional index such as the pain tolerance limit. When a mounted one-degree-of-freedom assistive robot was employed for the flexion and extension of the elbow joint, a general control method could be efficiently employed within a sufficiently safe range. This study also verified the concentration of contact force near the wrist and determined a guideline for improving the robot mechanism with less burden on the wearer. Thus, contact force distribution information can help evaluate structural problems.

This study contributes to improving the safety management performance of conventional wearable robots. The contents can be divided into three main categories. First, we developed a robot that can directly measure the distribution of contact forces between the robot and human body. Second, the application of contact force information in evaluating the safety of the control method in terms of the pain tolerance limit was demonstrated, in addition to developing a general safety management framework. Third, it was inferred that the contact force distribution information can help evaluate structural problems, and this is also a practical implication suggested by the experimental results.

However, sensor measurement performance and measurement limitations due to the robot's structure became apparent in this robot. In the future, we will study the measurement and control performance with a robot that cannot imitate the structure of the human body, such as the torso. Moreover, we will attempt to improve the robot such as frame design, joint locations, sensors used, including this arm-mounted type, based on the contact force distribution.

REFERENCES

[1] X. Gao, T. Yang, and J. Peng, "Logic-enhanced adaptive network-based fuzzy classifier for fall recognition in rehabilitation," *IEEE Access*, vol. 8, pp. 57105–57113, 2020.

[2] A. W. Boehler, K. W. Hollander, T. G. Sugar, and D. Shin, "Design, implementation and test results of a robust control method for a powered ankle foot orthosis (AFO)," in *Proc. IEEE Int. Conf. Robot. Autom.*, May 2008, pp. 2025–2030.

[3] A. Uehara, H. Kawamoto, and Y. Sankai, "Proposal of period modulation control of wearable cyborg HAL trunk-unit for Parkinson's disease/parkinsonism utilizing motor intention and dynamics," in *Proc. IEEE/SICE Int. Symp. Syst. Integr. (SII)*, Jan. 2023, pp. 1–6.

[4] *Annual Report on the Ageing Society [Summary] FY2021*, Cabinet Office Japan, Tokyo, Japan, Jul. 2021.

[5] M. Ide, T. Hashimoto, K. Matsumoto, and H. Kobayashi, "Evaluation of the power assist effect of muscle suit for lower back support," *IEEE Access*, vol. 9, pp. 3249–3260, 2021.

[6] K. Kong, J. Bae, and M. Tomizuka, "Control of rotary series elastic actuator for ideal force-mode actuation in human–robot interaction applications," *IEEE/ASME Trans. Mechatronics*, vol. 14, no. 1, pp. 105–118, Feb. 2009.

[7] T. Nef, M. Guidali, and R. Riener, "ARMin III—Arm therapy exoskeleton with an ergonomic shoulder actuation," *Appl. Bionics Biomech.*, vol. 6, no. 2, pp. 127–142, Jul. 2009, doi: 10.1080/11762320902840179.

[8] A. Montagner, A. Frisoli, L. Borelli, C. Procopio, M. Bergamasco, M. C. Carboncini, and B. Rossi, "A pilot clinical study on robotic assisted rehabilitation in VR with an arm exoskeleton device," in *Proc. Virtual Rehabil.*, Sep. 2007, pp. 57–64.

[9] R. Vertechy, A. Frisoli, A. Dettori, M. Solazzi, and M. Bergamasco, "Development of a new exoskeleton for upper limb rehabilitation," in *Proc. IEEE Int. Conf. Rehabil. Robot.*, Jun. 2009, pp. 188–193.

[10] P. D. Neuhaus, J. H. Noorden, T. J. Craig, T. Torres, J. Kirschbaum, and J. E. Pratt, "Design and evaluation of mina: A robotic orthosis for paraplegics," in *Proc. IEEE Int. Conf. Rehabil. Robot.*, Jun. 2011, pp. 1–8.

[11] R. J. Farris, H. A. Quintero, and M. Goldfarb, "Preliminary evaluation of a powered lower limb orthosis to aid walking in paraplegic individuals," *IEEE Trans. Neural Syst. Rehabil. Eng.*, vol. 19, no. 6, pp. 652–659, Dec. 2011.

[12] M. Talaty, A. Esquenazi, and J. E. Briceño, "Differentiating ability in users of the ReWalkTM powered exoskeleton: An analysis of walking kinematics," in *Proc. IEEE 13th Int. Conf. Rehabil. Robot. (ICORR)*, Jun. 2013, pp. 1–5.

[13] J. C. Perry, J. Rosen, and S. Burns, "Upper-limb powered exoskeleton design," *IEEE/ASME Trans. Mechatronics*, vol. 12, no. 4, pp. 408–417, Aug. 2007.

[14] T. Nef and R. Riener, "ARMin–design of a novel arm rehabilitation robot," in *Proc. 9th Int. Conf. Rehabil. Robot. (ICORR)*, 2005, pp. 57–60.
[15] M. Mihelj, T. Nef, and R. Riener, "ARMin II–7 DoF rehabilitation robot: Mechanics and kinematics," in *Proc. IEEE Int. Conf. Robot. Autom.*, Apr. 2007, pp. 4120–4125.
[16] C. Carignan, J. Tang, S. Roderick, and M. Naylor, "A configuration-space approach to controlling a rehabilitation arm exoskeleton," in *Proc. IEEE 10th Int. Conf. Rehabil. Robot.*, Jun. 2007, pp. 179–187.
[17] Y. Ren, H.-S. Park, and L.-Q. Zhang, "Developing a whole-arm exoskeleton robot with hand opening and closing mechanism for upper limb stroke rehabilitation," in *Proc. IEEE Int. Conf. Rehabil. Robot.*, Jun. 2009, pp. 761–765.
[18] M. Fontana, R. Vertechy, S. Marcheschi, F. Salsedo, and M. Bergamasco, "The body extender: A full-body exoskeleton for the transport and handling of heavy loads," *IEEE Robot. Autom. Mag.*, vol. 21, no. 4, pp. 34–44, Dec. 2014.
[19] N. Aphiratsakun and M. Parnichkun, "Balancing control of AIT leg exoskeleton using ZMP based FLC," *Int. J. Adv. Robotic Syst.*, vol. 6, no. 4, p. 34, Dec. 2009, doi: 10.5772/7250.
[20] K. A. Strausser and H. Kazerooni, "The development and testing of a human machine interface for a mobile medical exoskeleton," in *Proc. IEEE/RSJ Int. Conf. Intell. Robots Syst.*, Sep. 2011, pp. 4911–4916.
[21] F. Chen, Y. Yu, Y. Ge, and Y. Fang, "WPAL for human power assist during walking using dynamic equation," in *Proc. Int. Conf. Mechatronics Autom.*, Aug. 2009, pp. 1039–1043.
[22] Ü. Önen, F. M. Botsali, M. Kalyoncu, M. Tinkir, N. Yilmaz, and Y. Sahin, "Design and actuator selection of a lower extremity exoskeleton," *IEEE/ASME Trans. Mechatronics*, vol. 19, no. 2, pp. 623–632, Apr. 2014.
[23] D. Lee, I. Kang, D. D. Molinaro, A. Yu, and A. J. Young, "Real-time user-independent slope prediction using deep learning for modulation of robotic knee exoskeleton assistance," *IEEE Robot. Autom. Lett.*, vol. 6, no. 2, pp. 3995–4000, Apr. 2021.
[24] D. Sanz-Merodio, M. Cestari, J. C. Arevalo, X. A. Carrillo, and E. Garcia, "Generation and control of adaptive gaits in lower-limb exoskeletons for motion assistance," *Adv. Robot.*, vol. 28, no. 5, pp. 329–338, Mar. 2014, doi: 10.1080/01691864.2013.867284.
[25] R. Mendoza-Crespo, J. L. Gordillo, and R. Soto, "Wearable human lower limb prototype exoskeleton: An operative approach," in *Proc. 11th IEEE Int. Conf. Control Autom. (ICCA)*, Jun. 2014, pp. 267–272.
[26] I. Kang, D. D. Molinaro, S. Duggal, Y. Chen, P. Kunapuli, and A. J. Young, "Real-time gait phase estimation for robotic hip exoskeleton control during multimodal locomotion," *IEEE Robot. Autom. Lett.*, vol. 6, no. 2, pp. 3491–3497, Apr. 2021.
[27] J. Wang, X. Li, T.-H. Huang, S. Yu, Y. Li, T. Chen, A. Carriero, M. Oh-Park, and H. Su, "Comfort-centered design of a lightweight and backdrivable knee exoskeleton," *IEEE Robot. Autom. Lett.*, vol. 3, no. 4, pp. 4265–4272, Oct. 2018.
[28] K. Little, C. W. Antuvan, M. Xiloyannis, B. A. P. S. de Noronha, Y. G. Kim, L. Masia, and D. Accoto, "IMU-based assistance modulation in upper limb soft wearable exosuits," in *Proc. IEEE 16th Int. Conf. Rehabil. Robot. (ICORR)*, Jun. 2019, pp. 1197–1202.
[29] S. Yu, T.-H. Huang, D. Wang, B. Lynn, D. Sayd, V. Silivanov, Y. S. Park, Y. Tian, and H. Su, "Design and control of a high-torque and highly backdrivable hybrid soft exoskeleton for knee injury prevention during squatting," *IEEE Robot. Autom. Lett.*, vol. 4, no. 4, pp. 4579–4586, Oct. 2019.
[30] R. A. R. C. Gopura, K. Kiguchi, and Y. Li, "SUEFUL-7: A 7DOF upper-limb exoskeleton robot with muscle-model-oriented EMG-based control," in *Proc. IEEE/RSJ Int. Conf. Intell. Robots Syst.*, Oct. 2009, pp. 1126–1131.
[31] D. Lim, W. Kim, H. Lee, H. Kim, K. Shin, T. Park, J. Lee, and C. Han, "Development of a lower extremity exoskeleton robot with a quasi-anthropomorphic design approach for load carriage," in *Proc. IEEE/RSJ Int. Conf. Intell. Robots Syst. (IROS)*, Sep. 2015, pp. 5345–5350.
[32] J. Stein, K. Narendran, J. McBean, K. Krebs, and R. Hughes, "Electromyography-controlled exoskeletal upper-limb–powered orthosis for exercise training after stroke," *Amer. J. Phys. Med. Rehabil.*, vol. 86, no. 4, pp. 255–261, Apr. 2007.
[33] A. Foroutannia, M.-R. Akbarzadeh-T, and A. Akbarzadeh, "A deep learning strategy for EMG-based joint position prediction in hip exoskeleton assistive robots," *Biomed. Signal Process. Control*, vol. 75, May 2022, Art. no. 103557. [Online]. Available: https://www.sciencedirect.com/science/article/pii/S1746809422000799
[34] R. J. Sanchez, E. Wolbrecht, R. Smith, J. Liu, S. Rao, S. Cramer, T. Rahman, J. E. Bobrow, and D. J. Reinkensmeyer, "A pneumatic robot for re-training arm movement after stroke: Rationale and mechanical design," in *Proc. 9th Int. Conf. Rehabil. Robot. (ICORR)*, Jun. 2005, pp. 500–504.
[35] J. Klein, S. J. Spencer, J. Allington, K. Minakata, E. T. Wolbrecht, R. Smith, J. E. Bobrow, and D. J. Reinkensmeyer, "Biomimetic orthosis for the neurorehabilitation of the elbow and shoulder (BONES)," in *Proc. 2nd IEEE RAS EMBS Int. Conf. Biomed. Robot. Biomechatronics*, Oct. 2008, pp. 535–541.
[36] J. He, E. J. Koeneman, R. S. Schultz, H. Huang, J. Wanberg, D. E. Herring, T. Sugar, R. Herman, and J. B. Koeneman, "Design of a robotic upper extremity repetitive therapy device," in *Proc. 9th Int. Conf. Rehabil. Robot. (ICORR)*, Jun. 2005, pp. 95–98.
[37] M. Mochimaru, "Digital human models for human-centered design," *J. Robot. Mechtron.*, vol. 29, no. 5, pp. 783–789, 2017.
[38] *Physical Fitness and Athletic Ability Survey Report 2017*, Japan Sports Agency, Tokyo, Japan, Oct. 2018.
[39] *TRI Releases Wireless Version of 'SR Soft Vision'*, Tokai Rubber Ind., Ltd., Aichi, Japan, Mar. 2014. [Online]. Available: https://www.sumitomoriko.co.jp/pressrelease/2013/n51910098.pdf
[40] J. Gwak, M. Shino, and A. Hirao, "Early detection of driver drowsiness utilizing machine learning based on physiological signals, behavioral measures, and driving performance," in *Proc. 21st Int. Conf. Intell. Transp. Syst. (ITSC)*, Nov. 2018, pp. 1794–1800.
[41] T. Saito and H. Ikeda, "Measurement of human pain tolerance to mechanical stimulus of human-collaborative robots," *Specific Res. Rep. Nat. Inst. Ind. Saf.*, vol. 33, pp. 15–23, Jan. 2005.

SHINICHI MASAOKA (Member, IEEE) received the B.E. and M.E. degrees in electrical and electronic engineering and information engineering from Nagoya University, Japan, in 2020 and 2022, respectively. His research interest includes robotics.

YUKI FUNABORA (Member, IEEE) received the B.E., M.E., and Ph.D. degrees in electrical engineering and computer science from Nagoya University (NU), Japan, in 2007, 2009, and 2012, respectively. In 2012, he was a Postdoctoral Researcher with the RIKEN Advanced Science Institute, and since 2013, he has been an Associate Professor with NU. His research interests include human-cooperative robots, soft robotics, intelligent control, soft computing, and system design.

SHINJI DOKI (Senior Member, IEEE) received the B.E., M.E., and Ph.D. degrees in electronic-mechanical engineering from Nagoya University (NU), Japan, in 1990, 1992, and 1995, respectively. Since 2012, he has been a Professor with NU. His research interests include control, modeling, and signal/information processing and its application in motor drive systems. He was a recipient of the IEEE IECON '92 Best Paper Award, and awards from the FANUC FA and Robot Foundation and Institute of Electrical Engineers of Japan.